Solar Energy Materials & Solar Cells 95 (2011) 2357–2362

Contents lists available at ScienceDirect

Solar Energy Materials & Solar Cells

journal homepage: www.elsevier.com/locate/solmat

Low temperature Si doped ZnO thin films for transparent conducting oxides

J. Clatot [a], G. Campet [b], A. Zeinert [c], C. Labrugère [d], M. Nistor [e], A. Rougier [a,*]

[a] Laboratoire de Réactivité et de Chimie des Solides, UMR CNRS 6007, 33, rue Saint-Leu, 80039 Amiens, France
[b] CNRS, Université de Bordeaux, ICMCB, 87 avenue du Dr. A. Schweitzer, Pessac, F-33608, France
[c] Laboratoire de Physique de la Matière Condensée, Université de Picardie Jules Verne, 33 rue St. Leu, 80039, Amiens, France
[d] CeCaMA, Université de Bordeaux, ICMCB, 87 avenue du Dr. A. Schweitzer, Pessac, F-33608, France
[e] National Institute for Lasers, Plasmas and Radiation Physics, L22, PO Box MG-36, 77125 Bucharest-Magurele, Romania

ARTICLE INFO

Article history:
Received 11 January 2011
Accepted 1 April 2011
Available online 24 May 2011

Keywords:
Pulsed laser deposition
Transparent conducting oxide
Zinc oxide
Optical properties
Simulation

ABSTRACT

Si doped zinc oxide (SZO, Si 3%) thin films are grown at low substrate temperature ($T \leq 150$ °C) under oxygen atmosphere, using pulsed laser deposition (PLD). Si addition leads to film amorphization and higher densification. Hall effect measurements indicate a resistivity of $7.9 \times 10^{-4}\,\Omega$ cm for SZO thin films deposited at 100 °C under optimized 1.0 Pa oxygen pressure. This value is in good agreement with optical resistivity simulated from the transmittance spectra. XPS measurements suggest more than one oxygen environment, and a Si oxidation state lying in between 2 and 3 only. As a matter of fact, the values of both measured and simulated carrier numbers are smaller than the ones expected, assuming that all Si cations in the ZnO matrix are at the 4^+ oxidation state. Finally, the differences in the electrical and optical properties of SZO thin films deposited both on glass and PET substrates confirm the strong dependency of the electronic properties to the film crystallinity and stoichiometry in relationship with the substrate nature.

1. Introduction

Transparent conducting oxides (TCOs) are widely used in numerous new devices including flat panel display, solar cells and many optoelectronic applications [1]. Nowadays, the high demand for flexible optoelectronic devices requires the development of efficient (i.e. highly conducting and transparent in the visible domain) and non-costly TCOs deposited on polymer substrates. A TCO is a compromise between high transmittance and low resistivity [2,3]. Tin-doped indium oxide, ITO, is the most commonly used TCO, together with fluorine-doped tin oxide, FTO. However, the cost of In, and the high temperature needed for FTO deposition are limiting steps for the development of commercially available TCOs on plastic substrates. Doped ZnO thin films offer a promising alternative in particular for low temperature deposition [4]. Zinc oxide is cheap, abundant and non-toxic. Its wide band gap (E_g=3.30 eV) is correlated with transparency in visible range [5]. The substitutional doping of ZnO with group III metals such as Al, B and Ga via, for example, chemical vapor deposition (CVD) [6], magnetron sputtering [7–10] and pulsed laser deposition [11] was already reported. Herein, we investigate the influence of Si doping as potential 4^+ ionized donor center that would give two electrons to the conduction band, $2e^-$ (C.B.), in agreement with: $Zn^{2+}_{1-x}Si^{4+}_{x}O^{2-}[2e^-(C.B.)]$. In the literature, only few studies on 4^+ dopants are reported [12–14]. The interest of the ZnO:Si system was earlier pointed out by Minami et al., indicating a minimum resistivity of $3.8 \times 10^{-4}\,\Omega$ cm for Si doped ZnO thin films deposited below 250 °C using RF magnetron sputtering [13]. More recently, Das et al. [14] confirmed the promising performances (i.e. minimum resistivity value of $6.2 \times 10^{-4}\,\Omega$ cm) of Si doped ZnO thin films grown at 600 °C using sequential pulsed laser deposition. Searching for TCO layers with high performances to be later on incorporated in flexible devices, particular attention was devoted to low temperature deposition ($T \leq 150$ °C). ZnO:Si (SZO) thin films were grown by the pulsed laser deposition method on two types of substrates, glass and PET. Finally, the film electronic properties deduced from the simulation of the optical data are compared with electrical measurements.

2. Experimental

The Si doped ZnO targets, with a density higher than 80%, were prepared from a mixture of commercial ZnO, and SiO_2 powders annealed at T=1000 °C during 48 h. A 3% Si/Zn target molar ratio was initially used. SZO thin films were grown by pulsed laser deposition, PLD, using a KrF excimer laser beam (Lambda Physik Compex 102, λ=248 nm) with a laser fluence of 1–2 J cm^{-2}. The substrates were 1 cm^2 glass and polyethylene-terephthalate (PET)

* Corresponding author. Tel.: +33 5 40 00 62 63; fax: +33 5 40 00 27 61.
E-mail address: aline.rougier@u-picardie.fr (A. Rougier).

0927-0248/$ - see front matter © 2011 Elsevier B.V. All rights reserved.
doi:10.1016/j.solmat.2011.04.006

substrates. The base pressure in the chamber was in the order of 1.0×10^{-4} Pa. The depositions were performed in oxygen atmosphere in the $P_{O_2} = 1.0$ –10 Pa range and in vacuum. The substrate temperature varied from room temperature (RT) to 150 °C. The target substrate distance varied from 4 to 5 cm so that the substrate was set at the plume extremity. The duration of deposition lasted from a few minutes to 30 min with a repetition rate of 10 Hz. The thickness, determined by profilometry using a Dektak instrument, was estimated in the 300 nm range for sample deposited during 10 min corresponding to a high deposition rate of 5 Å s^{-1}. The morphology of the films was investigated by scanning electron microscopy (SEM) with a Philips XL 30 field emission gun FEG microscope. Their structure and crystallinity were examined by X-ray diffraction (XRD) using a D8 Bruker advance diffractometer (in the $\theta-2\theta$ configuration and λCuKα = 1.5409 Å). X-ray photoelectron spectroscopy (XPS) was performed on a VG 220i-XL ESCALAB spectrometer equipped with monochromatized AlKa source (1486.6 eV). Once deposited, thin films were kept under vacuum to prevent contamination. Thin films were exposed to air for few minutes in between their preparation on the substrate holder and their introduction into the spectrometer. All XPS spectra have been shifted to the C1s carbon pollution at 284.8 eV. The optical transmittance was measured using a CARY-5E Varian double beam, UV–vis-NIR spectrophotometer, between 250 and 2500 nm. The carrier type, concentration and mobility were determined with a MMR Technologies, Inc. Hall set up in the Van der Pauw geometry at a magnetic field of 0.3 T. The HRTEM imaging on SZO thin films deposited on Cu grids was performed using a FEI TECNAI F20 S-TWIN microscope.

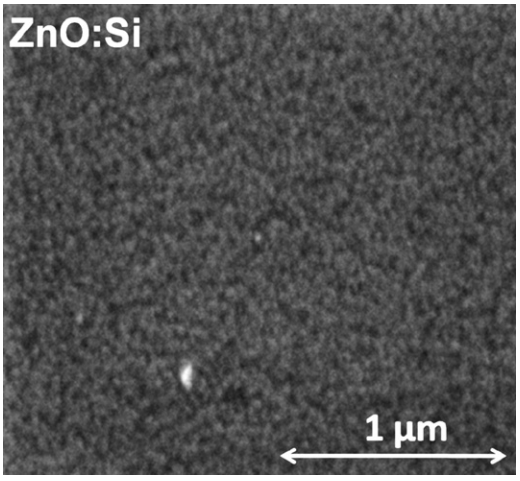

Fig. 1. SEM micrographs of 250 nm ZnO:Si (3%) thin films grown at room temperature under 1.0 Pa oxygen pressure.

3. Results and discussion

Our preliminary characterizations of undoped ZnO thin films demonstrate that films deposited under oxygen pressure below 1.0 Pa exhibit a metallic aspect making them unsuitable for applications as TCO. Therefore, SZO thin films deposited under oxygen pressure from 1.0 to 10 Pa were studied. At first glance, all SZO thin films are transparent.

3.1. Textural and structural characterizations

3.1.1. SEM analysis

The surface morphology of the SZO thin films appears homogenous and consists of small grains (Fig. 1). No significant influence of the substrate temperature was noticed whereas the film appears denser as oxygen pressure decreases. EDS analysis performed on SZO thin films deposited on sapphire substrate indicates a similar atomic Si/Zn ratio in the target and in the film (i.e. 3%).

3.1.2. XRD analysis

For films deposited at RT substrate, the evolution of XRD patterns with O_2 pressure in the 1.0–10 Pa range shows that only the SZO thin films deposited at 10 Pa are crystallized (Fig. 2a). In other words a decrease in oxygen pressure leads to film amorphization. Interestingly, using similar low P_{O_2} values, undoped ZnO thin films are crystallized (inset Fig. 2a). This observation suggests that all the Si atoms are not really substituted to Zn in the ZnO structure when $P_{O_2} < 10$ Pa and, so, the unsubstituted Si creates structural disorder leading to X-ray amorphization. Similar film amorphization with dopant addition was previously observed for other Al and Ga dopants [15]. At 10 Pa and RT, SZO thin films are polycrystalline with the hexagonal wurtzite structure (S.G. $P6_3mc$) and exhibit a (0 0 2) preferential orientation. An estimation of the *c*-parameter indicates that it is close to the value of undoped ZnO deposited in similar conditions ($c_{ZnO} = 5.22$ Å; $c_{SZO} = 5.23$ Å). Assuming that Si cations adopt a 4^+ oxidation state, a basic comparison of the ionic radii ($rSi^{4+} = 0.40$ Å $< rZn^{2+} = 0.74$ Å) cannot explain the slight increase in *c* parameter.

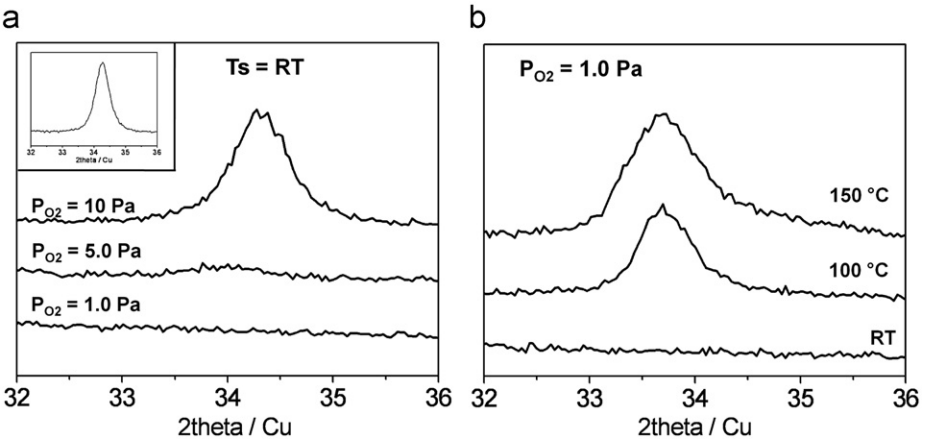

Fig. 2. X-ray diffraction patterns of 250 nm ZnO:Si (3%) thin films as a function (a) of the oxygen pressure of deposition ($P_{O_2} = 1.0$ Pa, 5.0 Pa, 10 Pa) for RT substrate (inset: XRD pattern of undoped ZnO thin films deposited at RT under 5.0 Pa oxygen pressure.), and (b) under 1.0 Pa oxygen pressure for RT, 100, and150 °C substrate temperature.

Such trend may be correlated to several parameters including a modification of the film stoichiometry (i.e. metal/O ratio) with Si addition or suggesting that part of all Si cations may exist in a lower oxidation state than 4^+; however, even so Si^{2+} and Si^{3+} cations exhibit smaller radii than Zn^{2+}. Therefore, we can reasonably evoke a slight oxygen substoichiometry (i.e. O/Zn(Si) < 1). In comparison, SZO thin films grown at 5.0 and 10 Pa are insulating, confirming the importance of oxygen deficiency for the conductivity. In the present study, regarding their insulating character, these films will not be investigated. Focusing on a 1.0 Pa growth pressure, the evolution of the XRD patterns with substrate temperature from RT to 150 °C is shown in Fig. 2b. For RT substrate, HRTEM analysis indicates that XRD amorphous SZO thin films are in fact (Fig. 3a) nanocrystallized, with crystallized domains in the order of 5 nm. An increase in substrate temperature is correlated to an increase in crystallinity, and, therefore, probably to an enhanced solubility of Si in ZnO matrix, according to our above reported considerations. SZO thin films remain textured with a (0 0 2) preferred orientation. For both films deposited at 100 and 150 °C, a very large *c* value of 5.31 Å is calculated from the (0 0 2) position. Such *c* increase as compared to bulk ZnO (c=5.21 Å) was already observed on undoped ZnO thin films grown in similar conditions (c=5.35 Å). Despite their surprisingly high value, the smaller *c* value recorded for SZO thin films is in good agreement with Si substitution. Overall, the large *c* value suggests a departure from the ideal ZnO (Zn/O=1) stoichiometry. Such increase in cell parameter may also express the presence of Zn in interstitial positions that would nevertheless be associated with an increase in the metallic aspect of the film that is not observed. The increase in film crystallinity with substrate temperature is also visible on the HRTEM micrographs, indicating crystallized domains of about 20 nm (Fig. 3b).

3.1.3. Optical characterization

Fig. 4 reports the optical transmittance spectra as a function of the substrate temperature. SZO thin films are transparent, with a transmittance higher than 80% (including glass substrate). A small decrease in transmittance is observed for films deposited at RT substrate. The optical gap can be extracted from the coefficient alpha with the following equation [16]:

$$\alpha h\nu = A(h\nu - E_g)^n \quad (1)$$

where A is a constant, E_g is the band gap of the material, and n=1/2 in case of direct gap or 2 for indirect gap. For our samples, the gap determination is obtained with a n=1/2, confirming that the gap is direct as known for pure ZnO. The optical band gap values as a function of the substrate temperature of deposition are gathered in Table 1. Independently of the substrate temperature, energy gap values are significantly higher than pure ZnO ($E_{g\ ZnO}$=3.30 eV) with a slight increase for 100 and 150 °C substrate temperatures. The increase in E_g with doping is well known as a result of the Burstein Moss (BM) effect that occurs in degenerate doped semiconductors [17]. As a matter of fact, the BM shift, ΔE_{BM} was calculated using the formula:

$$\Delta E_{BM} = \frac{\hbar^2}{2m_e^*}(3\pi n)^{2/3} \quad (2)$$

$$E_{BM} = E_0 + \Delta E_{BM} \quad (3)$$

while in Eq. (1), h and π are the usual constants, n is the electron density, and m_e^* is the effective mass. In Eq. (2), E_0 is the band gap of undoped ZnO taken at 3.30 eV at room temperature. An m_e^* of $0.2m_0$ leads to a ΔBM of 0.4 eV at RT and of 0.64 eV at 100 °C corresponding to optical gaps of E_g=3.70 eV (RT) and 3.94 eV (100 °C), respectively. The slight discrepancy with the E_g value determined from the transmittance spectra originates from the inaccuracy on the m_e^* value.

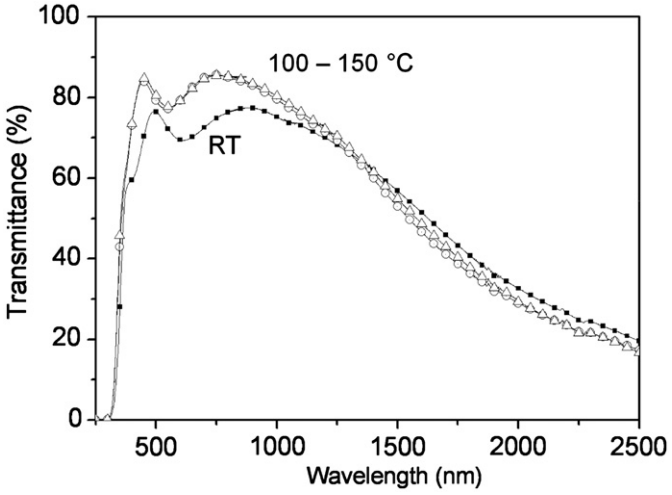

Fig. 4. Optical transmittance spectra for 250 nm ZnO:Si (3%) thin films deposited under 1 Pa oxygen pressure at RT, 100 and 150 °C.

Table 1
Evolution of the optical band gap as a function of the substrate temperature for ZnO:Si (3%) thin film deposited under 1.0 Pa oxygen pressure.

T_s (°C)	RT	100	150
E_g (eV)	3.70	3.86	3.84

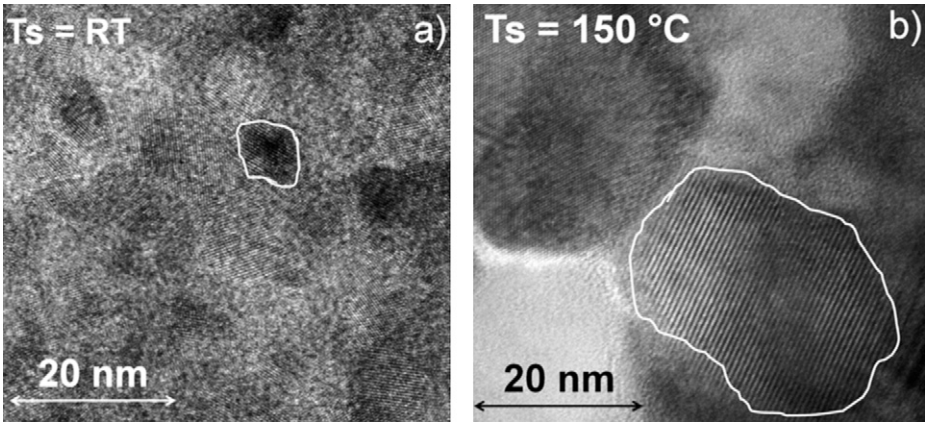

Fig. 3. High resolution transmission microscopy micrographs of ZnO:Si (3%) thin films deposited under 1.0 Pa oxygen pressure at RT (a) and 100 °C (b).

3.1.4. Hall measurements

As stated earlier, the electrical properties of the SZO thin films were studied using Hall effect measurements in the Van der Pauw geometry [18]. The evolution of the electrical resistivity with substrate temperature shows a slight decrease in resistivity with increasing substrate temperature reaching the lowest value of $7.9 \times 10^{-4}\,\Omega\,\mathrm{cm}$ for a 100 °C substrate temperature (Fig. 5). As expected, Hall effect measurements confirm the n-type character of the SZO thin films, with carrier concentrations in the 3.3

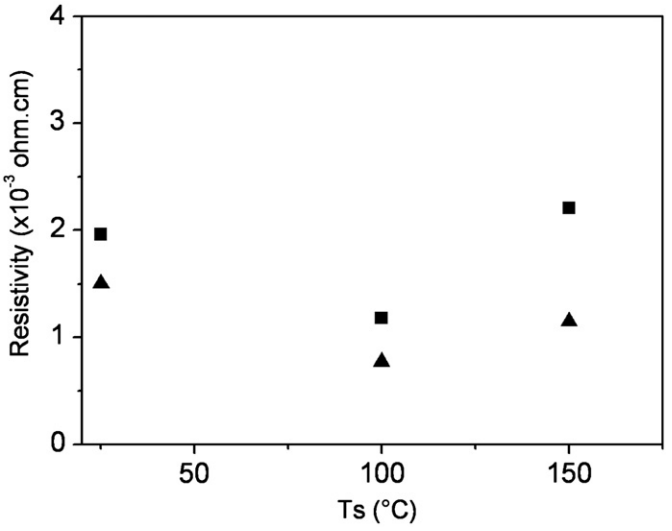

Fig. 5. Comparison of the resistivity measured by hall effect measurements (▲) and simulated from the optical transmittance spectrum (■) for 250 nm ZnO:Si (3%) thin films deposited under 1.0 Pa at RT, 100 and 150 °C.

(RT)–$6.6 \times 10^{20}\,\mathrm{cm}^{-3}$ (100 °C) range. Those values are smaller than the theoretical one, $N_{th.}$, calculated assuming that each Si gives two extra electrons in agreement with a 4^+ oxidation state and a crystal without defects (i.e. Si substituted on the Zn sites):

$$N_{th} = 0.03\frac{2\rho N_A}{M} \tag{4}$$

where ρ is the density ($\rho = 5.606 \times 10^{-3}\,\mathrm{kg\,cm}^{-3}$), N_A Avogadro constant ($N_A = 6.022 \times 10^{23}\,\mathrm{mol}^{-1}$), and M molar mass of ZnO ($M = 81.408 \times 10^{-3}\,\mathrm{kg\,mol}^{-1}$), 3% of theoretical Si.

A theoretical value $N_{th.}$ of $2.5 \times 10^{21}\,\mathrm{cm}^{-3}$ is calculated. Therefore, the experimental carrier concentration ($N = 3.3 - 6.6 \times 10^{20}\,\mathrm{cm}^{-3}$) corresponds to a concentration of 0.4–0.8% of active Si(4^+) in the ZnO structure. For all substrate temperatures, the electrical mobility is about $12\,\mathrm{cm}^2\,\mathrm{V}^{-1}\,\mathrm{s}^{-1}$.

The optical transmittance spectra were fitted with a commercial computer program (Code, W. Theiss [19]) using the following dielectric models:

(1) A Kim oscillator [20] to describe the interband transition of the absorption edge.
(2) A modified Drude model with frequency-dependent damping, which describes the intra-band transitions of the free electrons and takes into account possible electron scattering at ionized donors [21].

The optical properties of the glass substrate utilized in the modeling process were obtained from the separate measurement of a non-coated glass substrate. The comparison of the evolution of the resistivity (determined by optical measurements and electrical measurements) with substrate temperature shows a good agreement (Fig. 5). For both optical and electrical approaches, a minimum of resistivity is observed for SZO thin films deposited at 100 °C.

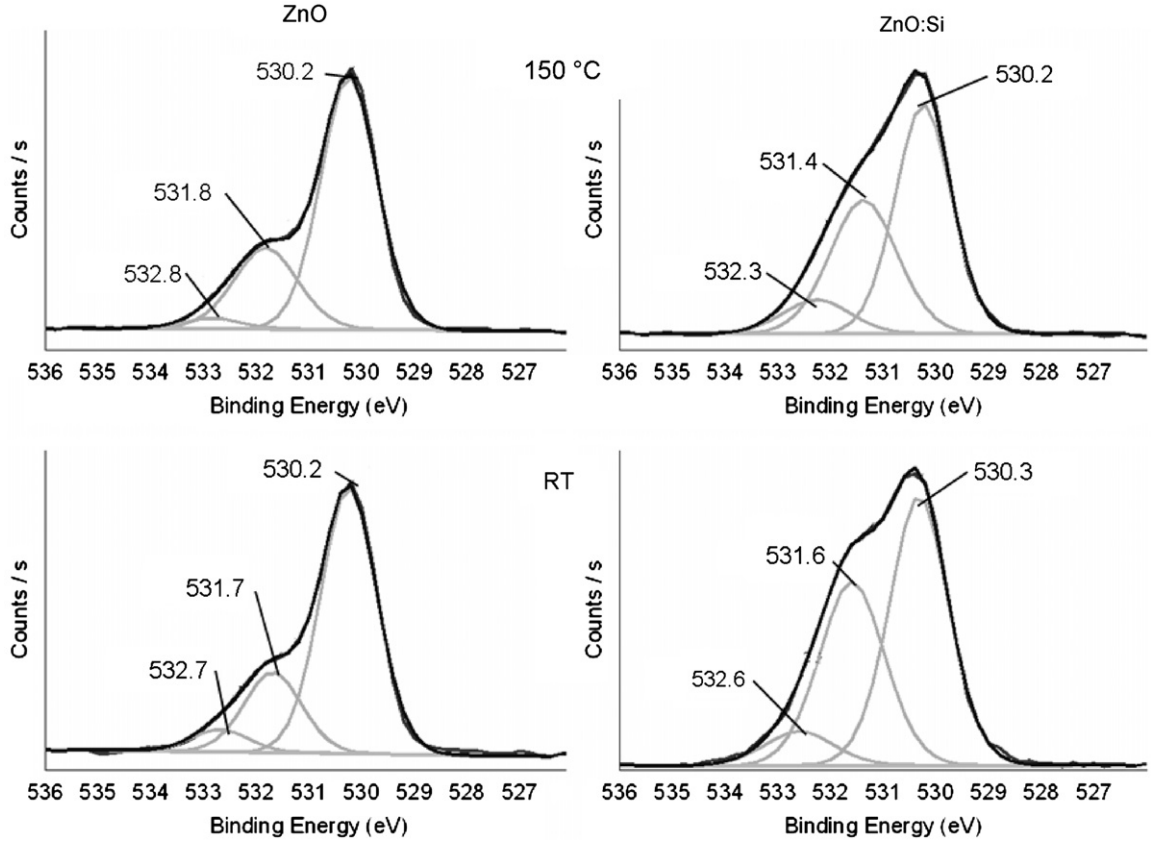

Fig. 6. O1s spectra of 250 nm ZnO and ZnO:Si (3%) thin films deposited under 1.0 Pa oxygen pressure as a function of the substrate temperature (RT, 150 °C).

Table 2
O1s Binding energies for ZnO and ZnO:Si (3%) thin film deposited under 1.0 Pa oxygen pressure at RT and 150 °C.

	ZnO			ZnO:Si (3%)		
Binding energy	***532.6 ± 0.2***	***531.6 ± 0.2***	***530.2 ± 0.1***	***532.6 ± 0.2***	***531.6 ± 0.2***	***530.2 ± 0.1***
RT	6%	22%	72%	7%	38%	55%
150 °C	3%	23%	74%	8%	34%	58%

3.1.5. XPS analysis

To further investigate the film stoichiometry, we carried out X-ray Photoelectron Spectroscopy analysis. For all samples, the level of carbon contamination lies in a similar 25–30 at% range The evolutions of the O1s XPS spectra of ZnO and SZO thin films as a function of the substrate temperature are compared in Fig. 6. Each spectrum can be fitted using three contributions, of which proportions are gathered in Table 2. The first one located at the binding energy of 530.2 ± 0.1 eV is assigned to oxygen atoms bound to Zn in ZnO [22]. The peak located at the highest energy of 532.6 ± 0.2 eV illustrates the C contamination and is more precisely attributed to C–O bonds. The intermediate peak, located in between, at 531.6 ± 0.2 eV, is the result of two contributions (i) the pollution corresponding to C=O bond (ii) and the presence of O^{2-} ions in the oxygen deficient regions within the ZnO matrix [23]. Interestingly, the intermediate peak is slightly shifted to lower binding energies for SZO thin films as compared to ZnO. For instance, for a 150 °C substrate temperature, it is shifted from 531.8 to 531.4 eV with Si addition. Such shift to lower binding energy is in favor of a stronger influence of the second contribution associated with the presence of oxygen deficient regions as compared to the C=O pollution. Besides, the proportion of the intermediate peak (Table 2) is overall much more significant than for ZnO thin films. This trend may suggest a larger amount of oxygen vacancies with Si addition. In fact, this increase in oxygen vacancies with Si addition in an oxygen deficient oxide film could be due to phase separation that could occur. It is known that in a mixture of SiO_x and ZnO, SiO_2 is formed at the expense of ZnO, [23] which becomes oxygen deficient; thus the formation of oxygen vacancies in the ZnO film doped with Si. This phenomenon is similar to a phase separation, which has been already observed in Al doped IZO [24] or ITO [25]. The presence of SiO_2 is under investigation using HRTEM/EDS characterization as it might be located at the grain boundaries. Similar XPS measurements were performed after 1 month of ageing in air. The overall shape of the spectra remains the same with an increase in the C contribution from 24 to 32 at%, suggesting an increase in surface pollution.

The XPS spectrum of the Si 2p core level is shown in Fig. 7. Surprisingly, the peak position, 102.4 eV, corresponds to a Si cation in a 2 to 3^+ oxidation state. A similar result, concluding on a lower oxidation state for Si than 4^+, was already reported by Das et al. [14]. The presence of 2^+ and 3^+ oxidation states would indicate that part of Si is electrically inactive whereas only one extra electron is donated by the 3^+ dopant. As a matter of fact, the experimental carrier concentration, namely N from 3.3 to $6.6 \times 10^{20}\,cm^{-3}$, does not correspond to a theoretical 3% of 3^+ dopant (Si^{3+}:$N_{th} = 1.2 \times 10^{21}\,cm^{-3}$), but only to half of it. Therefore, only 0.8–1.6% of Si^{3+} would be electrically active. Besides, a disorder environment, as favoured by Si addition, may induce a shift of the Si 2p position to lower binding energies. Therefore, the peak position of Si^{4+} would appear at lower values than 103.5 eV [26] as commonly reported for this oxidation state. To further characterize the Si oxidation state in SZO thin films, EELS experiments are currently in progress.

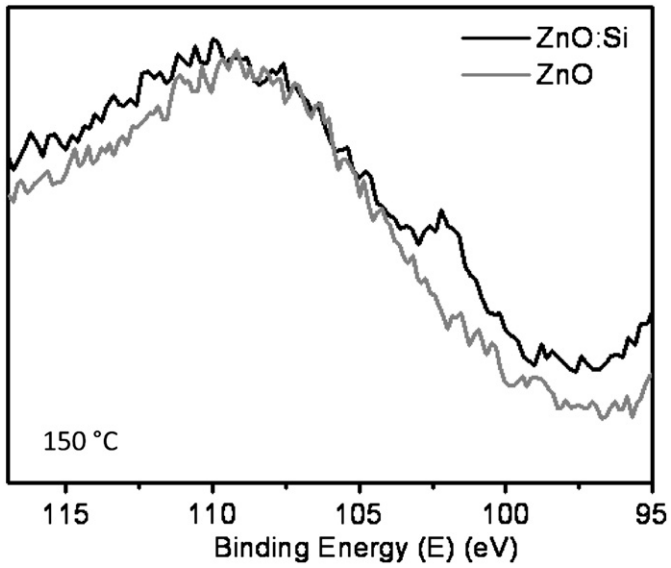

Fig. 7. Comparison of the 95–115 eV binding energy region corresponding to the Si 2p XPS spectrum location for ZnO and ZnO:Si (3%) thin films deposited under 1.0 Pa oxygen pressure at 150 °C.

3.1.6. Influence of the substrate nature

Finally, the influence of the substrate has been investigated. In particular, aiming at building flexible devices, SZO (3%) thin films were grown on PET substrate. Fig. 8 shows the transmittance curve of SZO thin film deposited on PET at 100 °C under 1.0 Pa of oxygen pressure. The transmittance curves on PET and glass are similar at the exception of the oscillations in near-IR region due to the PET substrate. These oscillations were simulated with 4 unidimensional oscillators. As an example the simulated optical parameters for the 100 °C SZO thin film deposited on glass and on PET are compared in Table 3. For both substrates, the resistivity values are similar in the order of $8 \times 10^{-4}\,\Omega$ cm. On the contrary, discrepancies in optical mobility and optical carrier concentration suggest an influence of the substrate nature on the film characteristics. Indeed, the comparison of the XRD patterns of SZO thin films deposited on glass and on PET substrate indicates a higher crystallinity on PET substrate associated with a slight shift of the X-ray peak position towards higher 2θ values (Fig. 9). A c parameter of 5.25 Å, smaller than the one determined for SZO on glass substrate of 5.31 Å, is estimated. In first approximation, it suggests a stoichiometry closer to the ideal one (i.e. $c = 5.21$ Å (Zn/O=1)). Due to the flexibility of the PET substrate, experimental Hall measurements of the electrical properties were unsuccessful.

4. Conclusion

Doped ZnO thin films offer a promising alternative to indium tin oxide (TCO) as transparent conductive layers. ZnO:Si (SZO) thin films were successfully deposited at low substrate temperature ($T \leq 150$ °C) under oxygen pressure using the pulsed laser

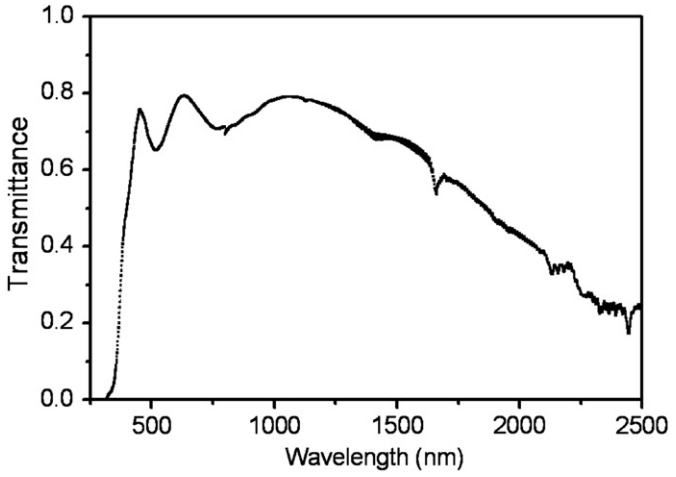

Fig. 8. Optical transmittance spectra for 350 nm ZnO:Si (3%) thin films deposited on PET substrate at 100 °C under 1 Pa oxygen pressure.

Table 3
Comparison of the simulated optical parameters, $N_{opt.}$, $\mu_{opt.}$, and $\rho_{opt.}$, for ZnO:Si (3%) deposited under 1.0 Pa oxygen pressure at 100 °C.

Best values	On glass	On PET
ρ_{opt} ($\times 10^{-4}\,\Omega$ cm)	7.9	9.0
μ_{opt} (cm^2 V^{-1} s^{-1})	9.8	15.0
N_{opt} ($\times 10^{20}$ cm^{-3})	8.9	4.6

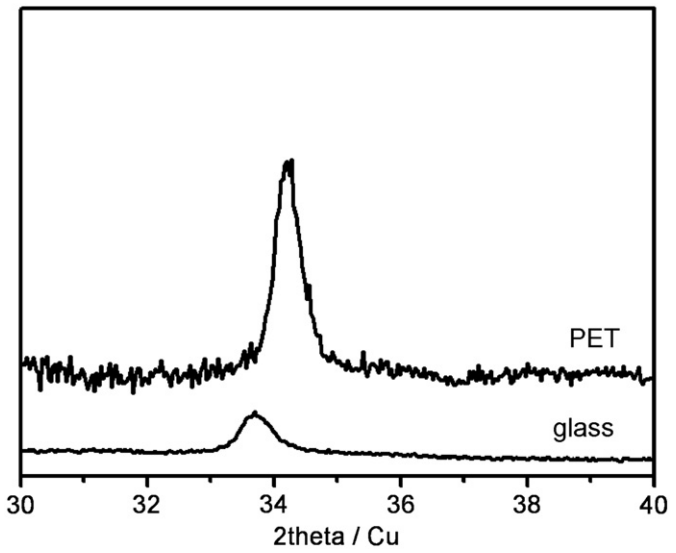

Fig. 9. Comparison of the XRD patterns of ZnO:Si (3%) thin film deposited on glass and on PET substrate at 100 °C under 1 Pa oxygen pressure.

deposition technique. SZO (3%) thin films deposited under 1 Pa of oxygen exhibit very promising resistivities of $8 \times 10^{-4}\,\Omega$ cm both for glass and PET substrates. Interestingly, the experimental carrier concentration does not correspond to the presence of Si^{4+} cations that would give two free electrons. Indeed XPS measurements confirm a lower Si oxidation state. The influence of the Si content on the electrical and optical properties will be reported in a forthcoming paper. Preliminary results confirm higher performances for SZO thin films with lower Si content (Si $\approx$ 1.0–1.5%). Besides, depositions on larger scale are in progress, indicating similar promising characteristics for high surface area SZO thin films.

Acknowledgments

The authors wish to thank Carine Davoisne (LRCS) for HRTEM measurements. The research leading to these results has received funding from the European Community's Seventh Framework Program (FP7) under grant agreement n_200431 (INNOSHADE).

References

[1] M.-I. Baraton, Int. J. Nanotechnol. Transparent conductive oxide materials: financial stakes and technological challenges 6 (9) (2009) 776–784.
[2] D.S. Ginley, H. Hosono, D.C. Paine (Eds.), Handbook of Transparent Conductors, Springer, New York, 2010
[3] Tadatsugu Minami, New n-type transparent conducting oxides, MRS Bulletin 25 (2000) 38–44.
[4] R. Triboulet, J. Perrière, Epitaxial growth of ZnO, Progress in Crystal Growth and Characterization of Materials 47 (2003) 65–138.
[5] Z.K. Tang, P. Yu, G.K.L. Wang, M. Kawasaki, A. Ohtomoto, H. Koinuma, Y. Segawa, Ultraviolet spontaneous and stimulated emissions from ZnO microcrystallite thin films at room temperature, Solid State Communications 103 (1997) 459–463.
[6] M. Shimizu, T. Shiosaki, A. Kawabata, Growth of *c*-axis oriented ZnO term thin films with high deposition rate on silicon by previous CVD method, Journal of Crystal Growth 57 (1982) 94–100.
[7] Z.-C. Jin, I. Hamberg, C.-G. Granqvist, Optical properties of sputter-deposited ZnO:Al thin films, Journal of Applied Physics 64 (10) (1988) 5117–5131.
[8] V. Assunção, E. Fortunato, A. Marquesa, H. Águasa, I. Ferreira, M.E.V. Costa, R. Martins, Influence of the deposition pressure on the properties of transparent and conductive ZnO:Ga thin-film produced by r.f. sputtering at room temperature, Thin Solid Films 427 (2003) 401–405.
[9] K. Ellmer, Resistivity of polycrystalline zinc oxide films: current status and physical limit, Journal of Physics D: Applied Physics 34 (2001) 3097–3108.
[10] K. Ellmer, A. Klein, B. Rech (Eds.), Transparent Conductive Zinc Oxide: Basics and Applications in Thin Film Solar Cells, Springer, Berlin, 2008
[11] J.P. Kim, S.-A. Lee, J.S. Bae, S.K. Park, U.C. Choi, C.R. Cho, Electrical properties and surface characterization of transparent Al-doped ZnO thin films prepared by pulsed laser deposition, Thin Solid Films 516 (2008) 5223–5226.
[12] M.R. Vaezi, S.K. Sadrnezhaad, Improving the electrical conductance of chemically deposited zinc oxide thin films by Sn dopant, Materials Science and Engineering B 141 (2007) 23–27.
[13] T. Minami, H. Sato, H. Nanto, S. Takata, Highly conductive and transparent silicon doped zinc oxide thin films prepared by RF magnetron sputtering, Japan Journal of Applied Physics 25 (1986) L776–L779.
[14] A.K. Das, P. Misra, L.M. Kukreja, Effect of Si doping on electrical and optical properties of ZnO thin films grown by sequential pulsed laser deposition, Journal of Physics D: Applied Physics 42 (2009) 165405–165412.
[15] J. Clatot, G. Campet, A. Zeinert, C. Labrugère, A. Rougier, Room temperature transparent conducting oxides based on zinc oxide thin films, Applied Surface Science (in press), doi:10.1016/j.apsusc.2010.12.010.
[16] J. Tauc, Optical Properties of Solids, vol. 22(Ed.)F. Abeles Amsterdam, North-Holland (1970) p. 903.
[17] E. Burstein, Anomalous optical absorption limit in InSb, Physical Review 93 (1954) 632–633.
[18] M. Nistor, F. Gherendi, N.B. Mandache, C. Hebert, J. Perrière, W. Seiler, Metal-semiconductor transition in epitaxial ZnO thin films, Journal of Applied Physics 106 (2009) 1037101–1037107.
[19] 〈http://www.wtheiss.com/〉.
[20] C.C. Kim, J.W. Garland, H. Abad, P.M. Raccah, Modeling the optical dielectric function of semiconductors: extension of the critical-point parabolic-band approximation, Physical Review B 45 (1992) 11749–11767.
[21] D. Mergel, Z. Qiao, Dielectric modelling of optical spectra of thin In_2O_3:Sn films, Journal of Physics D: Applied Physics 35 (2002) 794–801.
[22] A.C. Gâlcă, M. Secu, A. Vlad, J.D. Pedarnig, Optical properties of zinc oxide thin films doped with aluminium and lithium, Thin Solid Films 518 (2010) 4603–4606.
[23] J.M. Yuk, J.Y. Lee, Y. Kim, Y.S. No, T.W. Kim, W.K. Choi, Formation mechanisms of metallic Zn nanodots by using ZnO thin films deposited on n-Si substrates, Applied Physics Letters 97 (2010) 0619011–0619013.
[24] J. Sun, H. Gong, Abrupt resistivity decrease and other unexpected phenomena in a doped amorphous ternary metal oxide, Applied Physics Letters 97 (2010) 0921061–0921063.
[25] M. Nistor, J. Perrière, C. Hebert, W. Seiler, Nanocomposite indium–tin oxide films formation induced by a large oxygen deficiency, Journal of Physics: Condensed Matter 22 (2010) 0450061–0450067.
[26] Larisa P. Demyanova, A. Tressaud, Fluorination of alumino-silicate minerals: the example of lepidolite, Journal of Fluorine Chemistry 130 (2009) 799–805.